Effects of dispersion surfactants on the properties of ceramic – carbon nanotube (CNT) nanocomposites

Fawad Inam[1*], Andrew Heaton[2], Peter Brown[2], Ton Peijs[3], Michael J. Reece[3]

[1] Northumbria University, Faculty of Engineering and Environment, Ellison Building, Newcastle upon Tyne NE1 8ST, UK
[2] Dstl, Porton Down, Salisbury, Wiltshire SP4 0JQ, UK
[3] Queen Mary University of London, Nanoforce Technology Ltd and School of Engineering and Materials Science, Mile End Road, London E1 4NS, UK

* Corresponding author: fawad.inam@northumbria.ac.uk; Tel: 0044(0)191227 3741

Abstract
Gum Arabic (GA), Sodium Dodecyl Sulfate (SDS) and their mixture were used for the dispersion of multi-walled carbon nanotubes (CNTs) in an alumina matrix. A good dispersion at low loadings (0.5-1 wt%) of CNTs in alumina was achieved by an ultrasonic bath treatment. Dispersions were evaluated by UV-vis spectroscopy and agglomerate size analysis. The mixture of GA and SDS produced good dispersion as compared to GA and SDS alone. Nanocomposite powders were sintered by Spark Plasma Sintering (SPS). Microstructural, electrical and mechanical characterizations of sintered discs were carried out to evaluate the effectiveness of the different dispersants. The mixture of GA and SDS produced homogeneous and agglomerate-free CNT-alumina nanocomposites with higher electrical conductivity and indentation fracture toughness as compared to nanocomposites prepared using GA and SDS alone.

Keywords: A. Carbon nanotubes, A. Ceramic-matrix composites (CMCs), B. Electrical properties, B. Fracture toughness, E. Sintering.

1. Introduction

Carbon Nanotubes (CNTs) are one of the lightest [1], strongest [1,2] stiffest [1,3], electrically [4] and thermally [5] conductive engineering fibres. CNTs have already demonstrated their role as a multi-functional filler for various ceramic [6-12] and polymer [13-16] nanocomposites. However, CNT aggregation during processing of such nanocomposites is one of the major obstacles for their successful exploitation. This is due to the chemical inertness of CNTs caused by their unique

sp2 bonding in the graphene layers and their complex entanglement due to strong van der Waals forces, estimated at 500 eV/μm [17]. Such entangled bundles of CNTs cause significant reduction in the properties of ceramic nanocomposites [18]. Agglomerates of CNTs reduce the mechanical [13,19-21] and electrical properties [11,20] of various nanocomposites. To date, colloidal processing [22-24] has proven to be the most successful way of producing homogeneous suspensions of CNTs. Even in colloidal processing, there are many factors that influence CNTs de-bundling and homogenisation, such as the degree of bundling nanotubes, the dispersant/nanotube concentration ratio, the solvent dilution of the suspensions, the sonication and/or centrifugation parameters [25,26]. High energy ultrasonication is often used to disperse CNTs in ceramic matrices [6,22,24,25,27]. The selection of the dispersant is the very important to achieve good materials. Various organic solvents, such as, alcohols [11,12,22], benzene [28], DMF [22] have previously been used for de-bundling CNTs and homogeneously dispersing them in ceramic matrices. The use of such solvents may not be industrially up-scalable and environmental friendly. This demands the utilisation of less hazardous dispersants, like water-based solutions, for the dispersion of CNTs in ceramic matrices.

Gum Arabic (GA) [29-31] and Sodium Dodecyl Sulfate (SDS) [32-35] are the most commonly used amphiphilic water-soluble dispersants, which de-bundles CNT from their bundles by electrostatic and steric repulsions respectively [36]. Most of the previous research [32-35] has been focused on using single dispersant (mostly SDS) for making homogenised CNT solutions. Bandyopadhyaya *et al.* [31] reported that GA solution has better CNT dispersibility as compared to negatively charged SDS, positively charged cetyltrimethylammoniumchloride (CTAC) and dodecyltrimethylammoniumbromide (DTAB), non-ionic pentaoxoethylenedodecyl ether (C12E5), a polysaccharide (dextrin) and a long chain synthetic polymer poly(ethylene oxide) (PEO). Moon *et al.* [37] reported a zeta potential (ζ) of -27 mV and -21 mV for GA-CNT and SDS-CNT dispersions respectively. The absolute value for ζ should be >25 mV for achieving stable and fully-dispersed CNT suspension [37]. Wang *et al.* [38] improved the dispersion quality of toluene/water emulsions by coating CNTs with GA via interfacial trapping. For silicon nitride – CNT suspensions, the disentangling capability of GA was reported to be higher than SDS [25]. The authors concluded their findings solely on the basis of their microstructural observations [25]. Recently, Silva *et al.* [39] prepared alumina – CNT and zirconia – CNT nanocomposites by using surfactant based dispersants and reported good interface between the matrices and CNTs.

In this paper, we used GA, SDS and their mixture for dispersing CNTs in alumina matrix. The dispersion quality of various suspensions were characterised by UV-vis spectroscopy [40] and agglomerate size analyser [41]. After sintering, the dispersion of CNTs was analysed using high resolution electron microscopy. Indentation fracture toughness and electrical conductivities were measured to

compare the effect of different surfactants on the properties of ceramic-CNT nanocomposites.

2. Experimental

2.1. Starting materials

The CNTs used in this study are commercially available as “multi-walled carbon nanotubes (CNTs), NC-7000” from Nanocyl S.A., Belgium. They were synthesised by the catalytic CVD method and have an entangled cotton-like form. The CNTs have an average outer diameter of 9.5 nm (10 graphitic shells), lengths of up to 1.5 microns, purity of ~90% and density of 1.66 g/cm^3. An acid treatment was performed using a mixture of concentrated nitric (HNO_3, 90%) and sulfuric (H_2SO_4, 90%) acids. Distilled water (~20 vol%) was used to dilute the acids. In order to produce pure CNTs, the as-received CNTs (400 mg) were mixed with 200 ml dilute acidic solution. Both acids were equally mixed in the solution. The acid-CNT mixture was homogenized by stirring with a glass rod on heating plate (~85 ^oC) for 30 mins and then dispersed using ultrasonic bath treatment for 2 hrs. The resulting CNT dispersion was thoroughly washed with distilled water until the filtrate was colourless and neutral (pH ~7) after filtration. A Whatman filter paper of 1 µm was used. The purified CNTs were then dried for 48 hrs at 100 ^oC in an oven. CNTs were purified to >97% by acid treatment. Such purified CNTs improve mechanical properties of alumina-CNT nanocomposites [42]. The alumina matrix used in this study is commercially available “AKP 53 aluminum oxide” micropowder from Sumitomo, Japan. As supplied, the main features of this product are: alpha phase; D_{50}: 310 nm; purity: 99.99%; BET surface area 11.7 m^2/g; melting point 2050 ^oC; and density 3.97 g/cm^3. GA (51200, Fluka), SDS (L6206) and polyethylene glycol (PEG, 202436) were supplied by Sigma-Aldrich, UK.

2.2. Nanocomposite powder preparation and characterisations

CNTs were hand-mixed for 2 mins in SDS solution (0.25 g/l). The solution was dispersed in an ultrasonic bath for 6 hrs. To increase attraction between SDS coated CNTs (negatively charged) and alumina particles, alumina particles were mixed in PEG solution (0.5 g/l) for 30 mins to make them positively charged. Both liquids were mixed and then rotation ball milled for 8 hrs. The mixture was then dried at 80 ^oC for 12 hrs on a heating plate in air, followed by in a vacuum oven at 100 ^oC for 24 hrs. The dried agglomerated mixture was ground and sieved with a 250 mesh and then placed again in the vacuum oven at 100 ^oC for another 24 hrs to thoroughly extract the solvent. The same method was followed to prepare powder batches using distilled water only, GA solution (0.25 g/l) and GA/SDS solution (GA: 0.18 g/l and SDS: 0.07 g/l). Alumina – 0.5wt% CNT and alumina – 1 wt% CNT nanocomposite powders were prepared.

For agglomerate size analysis, CNTs were hand-mixed for 15 secs in the different solutions (100 mg/l) and the high power ultrasonicated for different durations. The solutions were then transferred to standard polycarbonate cuvettes (10x10x45mm)

and placed in a Malvern, Zetasizer nano-particle size analyzer (Nano ZS). Details of the technique are reported elsewhere [41]. The software was programmed to record the average of at least 30 readings for the quantification of the agglomerates size distribution. For UV-vis spectroscopy, CNTs were hand-mixed for 15 secs in different solution (12.5 mg/l) and high power ultrasonicated for 2 hrs. The solutions were then transferred to standard polycarbonate cuvettes (having zero UV-vis absorbance) and placed in a Perkin Elmer, Lambda 950 spectrophotometer. UV-vis spectroscopy was carried out for the wavelength range 400 to 800 nm. All of the above procedures were used for different dispersant solutions.

2.3. Spark Plasma Sintering (SPS)

Dried nanocomposite powder was poured into a graphite die and cold pressed at 0.6 MPa for 5 secs before sintering. Nanocomposite disks (thickness 3 mm and diameter 20 mm) were prepared by Spark Plasma Sintering (SPS) in a HPD 25/1 furnace (FCT Systeme, Germany). The sintering rate was 100 ^{o}C/min and maximum temperature was 1400 ^{o}C. A pressure of 50 MPa was applied in the range 1100-1200 ^{o}C and released at the end of the sintering time, which was 5 mins for all of the samples. The furnace has a pyrometer focused on a hole close to the sample in the upper punch to measure the processing temperature. Details of the SPS technique are reported elsewhere [43]. The same sintering procedure was used for all samples.

2.3. Nanocomposite characterisations

The spark plasma sintered (SPSed) samples were ground using SiC paper and diamond polished down to 1 micron. Density measurements were conducted using water buoyancy (Archimedes) method. SPSed samples were fractured in order to observe the grain size, and agglomeration and dispersion of CNTs. Fractured surfaces were gold coated and observed in a FE-SEM (FEI, Inspect F, 20 kV). Grain sizes were measured with the aid of the software (Image tool, v3, developed by UTSHCSA, USA). A minimum of 500 readings was taken to measure the grain sizes of each material. The electrical conductivity of the sintered materials was measured using the two-probe method [44] at room temperature. Silver electroded specimens (3 × 3 × 3 mm) were characterized (Equation 1) with a high sensitivity digital micro-ohmmetre (Keithley 580).

$$\sigma = \frac{l}{R \times A} \qquad \text{Equation 1}$$

Where, σ = electrical conductivity, l = sample thickness (3 mm), R = electrical resistance and A = cross-sectional area (9 mm^2). The Vickers indentation method was used to measure hardness and indentation fracture. A diamond indenter was applied to the surface of the specimens. A load of 2.5 kg was used for a duration time of 5 secs. Vickers hardness was evaluated in accordance with ASTM C1327-

03. For indentation fracture toughness Evans and Charles' semi-empirical formula [45] was used (Equation 2).

$$IFT = 0.16H\sqrt{a}\left(\frac{c}{a}\right)^{-3/2} \qquad \text{Equation 2}$$

Where, IFT = indentation fracture toughness, a = indentation half diagonal length and c = mean radial crack length.

3. Results and Discussion

3.1. Agglomerate size analysis and UV-vis spectroscopy

CNTs were separately ultrasonicated for various durations and their agglomerate sizes were then measured immediately (Figure 1). This agglomeration is particularly significant in CVD-grown nanotubes because substantial entanglement of the tubes occurs during nanotube synthesis [44]. For all of the ultrasonication durations, GA+SDS solution disperses CNTs more efficiently as compared to SDS solution and GA solutions alone (Figure 1).

The value of absorbance at a specific wavelength is proportional to the amount of de-bundled CNTs [40]. Figure 2 shows the UV-vis spectra of different CNTs solutions. A major absorbance peak was observed in the range 525-565 nm. Grossaid *et al.* [40] reported that the exact and absolute value of the absorbance at a certain wavelength corresponds to the superposition of different electronic transitions of different kinds of CNTs. It is not possible to attribute one peak of the spectrum to a specific kind of CNT in the range of wavelengths considered [40]. However, it is clear that GA+SDS solution disperses CNTs more efficiently as compared to SDS solution and GA solution alone (Figure 2). It should be noted that results (Figure 1 and 2) presented here are for comparison only and do not involve the optimum conditions for dispersing the CNTs.

3.2. FE-SEM analysis

Fully densified materials (~100% theoretical density) were sintered using an SPS furnace without damaging the CNTs [46]. Representative images of the fractured surfaces of the SPSed alumina and nanocomposites were selected for studying the distribution of the CNTs (Figure 3). Residual porosity and large grains (2.72 ± 0.87 μm) were observed for alumina (Figure 3a). CNTs improved densification and retarded grain growth in alumina nanocomposites (Figure 3b-d), which was the subject of our previous study [47]. Bright micron-sized aggregates of CNTs are visible in the sample prepared using SDS solution as the dispersant (Figure 3b). The presence of these aggregates contributes to grain coarsening during sintering and produces non-uniformity in the resulting microstructure [48]. The sample prepared using GA solution as the dispersant has a homogeneous distribution of individual CNTs (Figure 3c). A finer grain size was observed when SDS+GA solution was used for dispersing and mixing CNTs with alumina. Such a fine grain size indicates better homogenization and de-bundling of CNTs in alumina. Those

prepared with SDS+GA solution have a grain size of 360 ± 50 nm (Figure 3d) compared to the equivalent composite prepared with GA solution alone (grain size: 456 ± 74 nm).

3.2. Electrical and mechanical properties

The electrical conductivities (Figure 4) and indentation fracture toughness (Figure 5) were measured to evaluate the effectiveness of the different dispersant solutions on homogenisation. Error bars are not marked in the electrical conductivity measurements, as they are very small (Figure 4). Alumina is inherently an electrical insulator (conductivity: ~10^{-13} S/m). To achieve a low percolation threshold and high electrical conductivity for alumina-CNT nanocomposite, a good dispersion of CNTs is a prerequisite. Nanocomposites prepared using distilled water showed lower electrical conductivities as compared to SDS, GA and SDS+GA solutions. The highest electrical conductivity (S/m) was observed for alumina-CNT nanocomposites prepared using SDS+GA solution.

Indentation fracture toughness evaluates the ability of a material to resist crack propagation under contact loading. Different toughening mechanism are reported for ceramic-CNT nanocomposites: crack deflection at the CNT-ceramic matrix interface [12,49,50]; crack bridging by CNTs [49,50]; CNT pullout [49,50] and CNT shear band collapse [50]. To optimise the effectiveness of these mechanisms, it is necessary to homogenously distribute the CNTs in the ceramic nancomposite. As compared to nanocomposites prepared by SDS solution and GA solution, increased fracture toughness (32% and 22%, respectively) was observed for the nanocomposite prepared by SDS+GA solution. It should also be noted that the nanocomposites prepared using GA solutions, possess higher electrical conductivities and indentation fracture toughness as compared to SDS solution. Hence it is concluded that GA is a better dispersing agent for CNTs in an aqueous solution, which was also reported by Bandyopadhyaya *et al.* [31]. For SDS alone, negatively charged sulphate groups coat CNTs which provide electrostatic repulsion, and thus prevent aggregation [51,52]. For GA, the long polymer chains of GA physically get adsorbed between CNTs that disperses them by steric repulsion [31,53]. Hence it is proposed that for the SDS+GA solution, both mechanisms are responsible for de-bundling of CNTs and homogeneously mixing them with alumina powder. The increased electrical conductivity (Figure 4) and fracture toughness (Figure 5) are the result of such improved dispersion of CNTs in alumina.

4. Conclusion

For the successful exploitation of ceramic-CNT nanocomposites, the homogenous dispersion and distribution of the CNTs in the ceramic matrices remains crucial. A new, environmentally friendly and industrial scalable, method has been developed to produce ceramic-CNT nanocomposites. From agglomerate size analysis and UV-vis spectroscopy, it is clear that GA+SDS produces fine and homogenous CNT

dispersions. Sintered nanocomposites prepared from these GA+SDS solutions, showed no evidence of aggregation and a good distribution of the CNTs were observed. Those nanocomposites showed higher electrical conductivity and indentation fracture toughness as compared to those prepared using GA and SDS dispersions alone. In GA+SDS solution, it is proposed that both mechanisms (electrostatic and steric repulsions) for de-agglomeration of CNTs are operative. Such repulsions are responsible for improved dispersion and homogenous mixing of CNTs in alumina. The dispersing effect of various solutions for making good ceramic-CNT nanocomposites was found to be in the order of SDS+GA>GA>SDS>water.

Acknowledgement

The authors would like to acknowledge Dstl, Ministry of Defence (UK) for their financial support (contract no. DSTLX-1000026924).

References

[1] Zhang X, Li Q, Holesinger TG, Arendt PN, Huang J, Kirven PD, et al. Ultrastrong, stiff, and lightweight carbon-nanotube fibers. Adv Mater 2007;19(23):4198–201.
[2] Barber AH, Andrews R, Schadler LS, Wagner HD. On the tensile strength distribution of multiwalled carbon nanotubes. Appl Phys Lett 2005;87(20):203106.
[3] Treacy MMJ, Ebbesen TW, Gibson JM. Exceptionally high Young's modulus observed for individual carbon nanotubes. Nature 1996;381(6584):678–80.
[4] Tawfick S, O'Brien K, Hart AJ. Flexible high-conductivity carbon-nanotube interconnects made by rolling and printing. Small 2009;5(21):2467–73.
[5] Berber S, Kwon YK, Tománek D. Unusually high thermal conductivity of carbon nanotubes. Phys Rev Lett 2000;84(20):4613–6.
[6] Inam F, Yan H, Peijs T, Reece MJ. Electrically conductive alumina–carbon nanocomposites prepared by spark plasma sintering. J Eur Ceram Soc 2010;30(2):153–7.
[7] White AA, Best SM, Kinloch IA. Hydroxyapatite–carbon nanotube composites for biomedical applications: a review. Int J Appl Ceram Tech 2007;4(1):1–13.
[8] Arvantelis C, Jayaseelan DD, Cho J, Boccaccini AR. Carbon nanotubes–SiO2 composites by colloidal processing. Adv Appl Ceram 2008;107(3):155–8.
[9] Dusza J, Blugan G, Morgiel J, Kuebler J, Inam F, Peijs T, et al. Hot-pressed and spark plasma sintered zirconia/carbon nanofiber composites. J Eur Ceram Soc 2009;29(15):3177–84.
[10] Gao L, Jiang L, Sun J. Carbon nanotube-ceramic composites. J Electroceram 2006;17(1):51–5.
[11] Zhan GD, Kuntz JD, Garay JE, Mukherjee AK. Electrical properties of nanoceramics reinforced with ropes of single-walled carbon nanotubes. Appl Phys Lett 2003;83(6):1228–30.
[12] Zhan GD, Kuntz JD, Wan J, Mukherjee AK. Single-wall carbon nanotubes as attractive toughening agents in alumina-based nanocomposites. Nat Mater 2003;2(1):38–42.
[13] Inam F, Wong DYW, Kuwata M, Peijs T. Multiscale hybrid micro-nanocomposites based on carbon nanotubes and carbon fibers. J Nanomater 2010;2010: 453420.
[14] Deng H, Zhang R, Bilotti E, Peijs T. A novel concept for highly oriented carbon nanotubes composite tapes or fibres with high strength and electrical conductivity. Macromol Mater Eng 2009;294(11):749–55.
[15] Zhang R, Baxendale M, Peijs T. Universal resistivity-strain dependence of carbon nanotube/polymer composite. Phys Rev B 2007;76(19):195433.

[16] Wang Z, Ciselli P, Peijs T. The extraordinary reinforcing efficiency of single walled carbon nanotubes in oriented poly(vinyl alcohol) tapes. Nanotechnology 2007;18(45):455709.
[17] Thess A, Lee R, Nikolaev P, Dai H, Petit P, Robert J, , et al. Crystalline ropes of metallic carbon nanotubes. Science 1996;273(5274):483–7.
[18] Cho J, Boccaccini AR, Shaffer MSP. Sintering ceramic matrix composites containing carbon nanotubes. J Mater Sci 2009;44(8):1934–51.
[19] Ning J, Zhang J, Pan Y, Guo J. Surfactants assisted processing of carbon nanotube-reinforced SiO^2 matrix composites. Ceram Int 2004;30(1):63–7.
[20] Service RF. Superstrong nanotubes show they are smart, too. Science 1998;281(5379):940–2.
[21] Eitan A, Fisher FT, Andrews R, Brinson LC, Schadler LS. Reinforcement mechanisms in MWCNT-filled polycarbonate. Compos Sci Technol 2006;66(9):1162–73.
[22] Inam F, Yan H, Reece MJ, Peijs T. Dimethylformamide: an effective dispersant for making ceramic–carbon nanotube composites. Nanotechnology 2008;19(19):195710.
[23] Sun J, Gao L, Li W. Colloidal processing of carbon nanotube/alumina composites. Chem Mater 2002; 14(12):5169-72.
[24] Poyato R, Vasiliev AL, Padture NP, Tanaka H, Nishimura T. Aqueous colloidal processing of single-wall carbon nanotubes and their composites with ceramics. Nanotechnology 2006;17(6):1770–7.
[25] Belmonte M, Vallés C, Maser WK, Benito AM, Martinez MT, Miranzo P, Osendi MI. Processing route to disentangle multi-walled carbon nanotube towards ceramic composite. J Nanosci Nanotechnol 2009;9(10):6164–70.
[26] Tan Y, Resasco DE. Dispersion of single-walled carbon nanotubes of narrow diameter distribution. J Phys Chem B 2005;109(30), 14454–60.
[27] Balázsi C, Sedláčková K, Czigány Z. Structural characterization of Si_3N_4–carbon nanotube interfaces by transmission electron microscopy. Compos Sci Technol 2008;68(6):1596–9.
[28] Chen ML, Zhang FJ, Oh WC. Photocatalytic degradation of methylene blue by CNT/TiO_2 composites prepared from MWCNT and titanium n-butoxide with benzene. J Kor Ceram Soc 2008;45(11):651–7.
[29] Picton L, Bataille I, Muller G. Analysis of a complex polysaccharide (gum arabic) by multi-angle laser light scattering coupled on-line to size exclusion chromatography and flow field flow fractionation. Carbohydr Polym 2000;42(1):23–31.
[30] Benton W. Encyclopedia Britannica 1966;257-9 (Britannica, Chicago)
[31] Bandyopadhyaya R, Roth EN, Regev O, Rozen RY. Stabilization of individual carbon nanotubes in aqueous solutions. Nano Lett 2002;2(1):25–8.
[32] Fan J, Zhao D, Wu M, Xu Z, Song J. Preparation and microstructure of multi-wall carbon nanotubes-toughened Al_2O_3 composite. J Am Ceram Soc 2006;89(2):750–3.
[33] Lu K. Freeze cast carbon nanotube-alumina nanoparticle green composites. J Mater Sci 2008;43(2):652–9.
[34] Ciselli P. The potential of carbon nanotubes in polymer composites. PhD thesis 2007, Eindhoven University of Technology, The Netherlands.
[35] Regev O, Elkati PNB, Loos J, Koning CE. Preparation of conductive nanotube-polymer composites using latex technology. Adv Mater 2004;16(3):248–51.
[36] Bulatovic SM. Handbook of flotation reagents 2007, vol 1 (Elsevier, UK)
[37] Moon JS, Park JH, Lee TY, Kim YW, Yoo JB, Park CY, et al. Transparent conductive film based on carbon nanotubes and PEDOT composites. Diamond Relat Mater 2005;14(11-12):1882–7.
[38] Wang RK, Park HO, Chen WC, Batista CS, Reeves RD, Butler JE, et al. Improving the effectiveness of interfacial trapping in removing single-walled carbon nanotube bundles. J Am Chem Soc 2008;130(44):14721–8.

[39] Silva PR, Almeida VO, Machado GB, Benvenutti EV, Costa TMH, Gallas MR. Surfactant-based dispersant for multiwall carbon nanotubes to prepare ceramic composites by a sol-gel method. Langmuir 2012;28(2):1447–52.
[40] Grossiord N, Regev O, Loos J, Meuldijk J, Koning CE. Time-dependent study of the exfoliation process of carbon nanotubes in aqueous dispersions by using UV-visible spectroscopy. Anal Chem 2005;77(16):5135–9.
[41] Inam F, Peijs T. Re-aggregation of carbon nanotubes in two-component epoxy system. J Nanostruct Polym Nanocomp 2006;2(3):87–95.
[42] Yamamoto G, Hashida T, Omori M, Kimura H. Reinforcement of alumina with surface modified carbon nanotubes. Mater Sci Forum 2010;631-632:231–6.
[43] Orru R, Licheri R, Locci AM, Cincotti A, Cao G. Consolidation/synthesis of materials by electric current activated/assisted sintering. Mater Sci Eng R 2009;63(4-6):127–287.
[44] Thostenson ET, Karandikar PG, Chou TW. Fabrication and characterization of reaction bonded silicon carbide / carbon nanotube composites. J Phys D: Appl Phys 2005:38(21);3962–5.
[45] Evans AG, Charles EA. Fracture toughness determination by indentation. J Am Ceram Soc 1976;59(7-8):371–2.
[46] Inam F, Yan HX, Reece MJ, Peijs T. Structural and chemical stability of multiwall carbon nanotubes in sintered ceramic nanocomposite. Adv Appl Ceram 2010. DOI: 10.1179/174367509X12595778633336 (2010).
[47] Inam F, Yan HX, Peijs T, Reece MJ. The sintering and grain growth behaviour of ceramic-carbon nanotube nanocomposites. Compos Sci Technol 2010;70(6):947–52.
[48] Tamburini UA, Garay JE, Munir ZA. Fast low-temperature consolidation of bulk nanometric ceramic materials. Scr Mater 2006:54(5):823–8.
[49] Guo S, Sivakumar R, Kagawa Y. Multiwall carbon nanotube-SiO_2 nanocomposites: sintering, elastic properties, and fracture toughness. Adv Eng Mater 2007;9(1-2):84–7.
[50] Xia Z, Riester L, Curtin WA, Li H, Sheldon BW, Liang J, et al. Direct observation of toughening mechanisms in carbon nanotube ceramic matrix composites. Acta Mater 2004;52(4):931–44.
[51] Jiang L, Gao L, Sun J. Production of aqueous colloidal dispersions of carbon nanotubes. J Colloid Interface Sci 2003;260(1):89–94.
[52] Strano MS, Moore CM, Miller MK, Allen MJ, Haroz EH, Kittrel C, et al. The role of surfactants adsorption during ultrasonication in the dispersion of single-walled carbon nanotubes. J Nanosci Nanotechnol 2003;3(1-2):81–6.
[53] de Gennes PG. Simple views on adhesion and fracture. Can J Phys 1990;68(9):1049–54.

List of figures

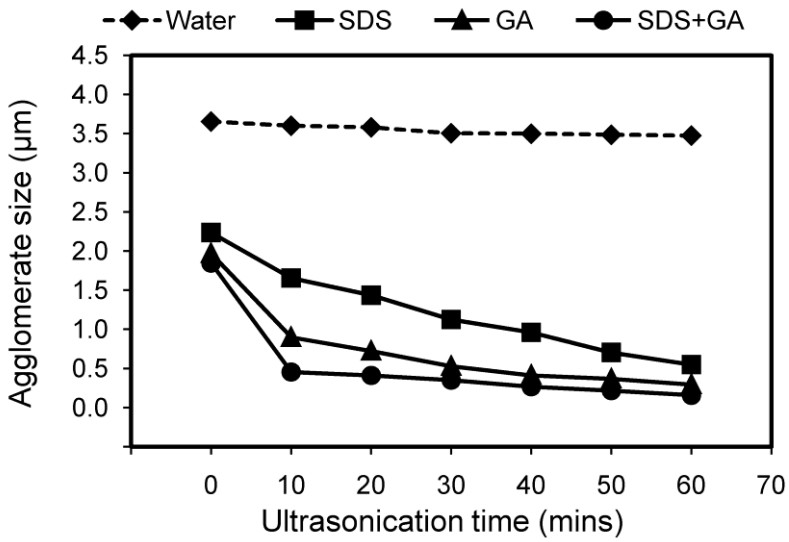

Figure 1. Agglomerate size analysis with respect to ultrasonication time in different solutions (CNT concentration: 100 mg/l).

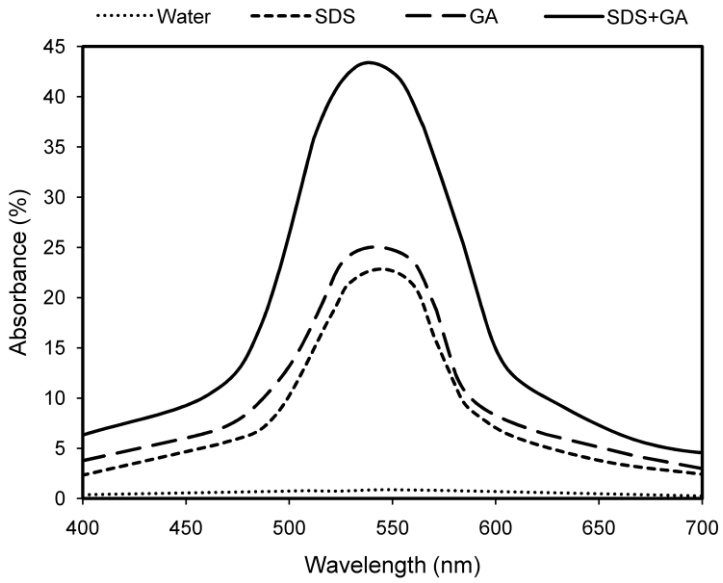

Figure 2. UV-vis spectra of different aqueous solutions (CNT concentration: 12.5 mg/l).

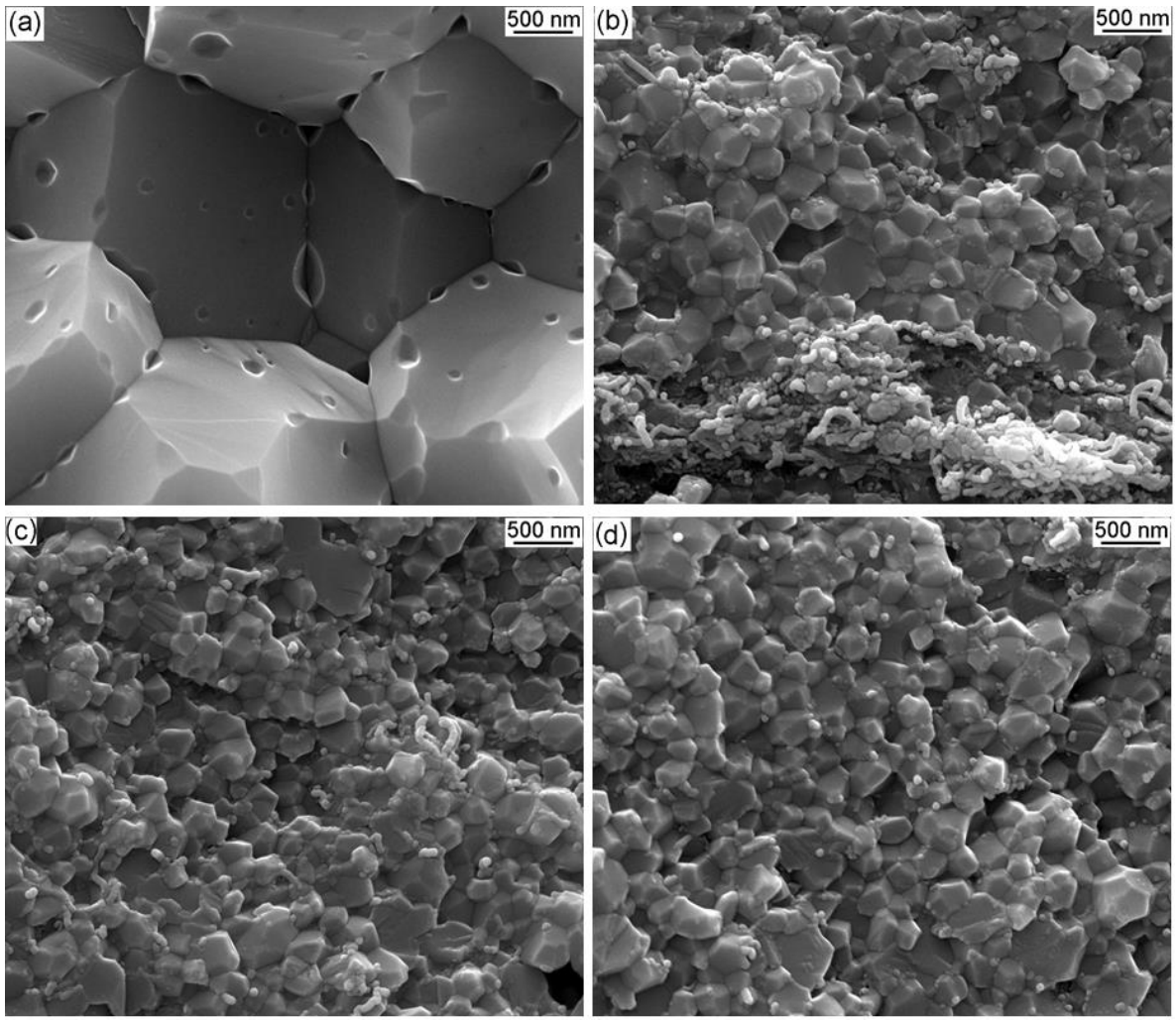

Figure 3. Field-Emission Scanning Electron Microscopy (FE-SEM) of fractured surfaces of sintered materials. SPSed at 1400 ^{o}C/ 50 MPa for 3 mins: a) alumina; b) alumina + 1wt% CNTs, dispersed in SDS solution; c) alumina + 1wt% CNTs, dispersed in GA solution; and d) alumina + 1wt% CNTs, dispersed in SDS+GA solution.

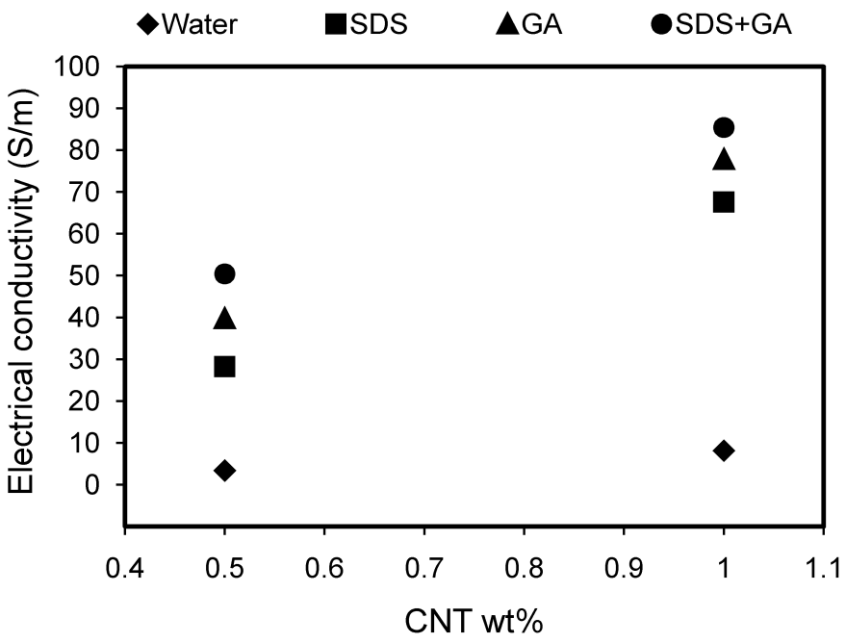

Figure 4. Electrical conductivites of alumina-CNT nancomposites, prepared using different dispersant solutions. Electrical conducivity of alumina is ~10^{-13} S/m.

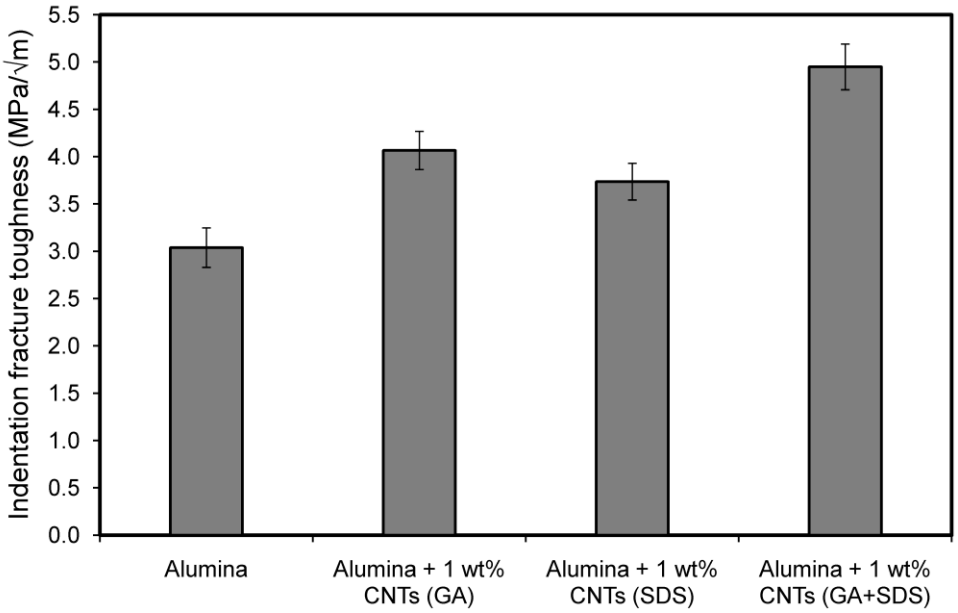

Figure 5. Indentation fracture toughness of sintered materials.